

Phasing Trajectories to Deploy a Constellation in a Halo Orbit

Chen, Hongru

Key Laboratory of Space Utilization, Technology and Engineering Center for Space Utilization,
Chinese Academy of Sciences

Ma, Jian

Key Laboratory of Space Utilization, Technology and Engineering Center for Space Utilization,
Chinese Academy of Sciences

<https://hdl.handle.net/2324/4481566>

出版情報 : Journal of Guidance, Control, and Dynamics. 40 (10), pp.2662-2667, 2017-10. American
Institute of Aeronautics and Astronautics

バージョン :

権利関係 :



Phasing Trajectories to Deploy a Constellation in a Halo Orbit

Hongru Chen^{*,1} and Jian Ma^{1,2}

¹*Key Laboratory of Space Utilization, Technology and Engineering Center for Space Utilization, Chinese Academy of Sciences, Beijing, China 100094*

²*University of Chinese Academy of Sciences*

I. Introduction

Strategies for deploying satellite constellations in the two-body problem have been extensively studied and applied, whereas the present Note concerns deploying a constellation in the three-body problem. Motivated by a proposed CubeSat project PHOEBE (Positioning using earth-moon Halo Orbit Experimental BEacons) for positioning the users on the far side of Moon [1], this study investigates methods of designing the phasing trajectory to deploy a constellation in a halo orbit with low Δv . The halo orbit is a three-dimensional periodic orbit about a libration point in the three-body system.

There will be missions aimed at the far side of the Moon in the near future [2]. The terrain and resources on the far side of the Moon are very different from those on the near side. In addition, the far side is an ideal platform for radio astronomy since the Moon can shield radio noises from the Earth. China will land the Chang'E-4 on the far side in 2018 [3]. However, challenges for navigation and communication arise, as the far side is invisible to the Earth. Moreover, as the terrain on the far side is very rough, the requirement of landing accuracy is even strict. Hill and Born [4], and Hesar et al. [5] have studied the technique of tracking the satellites in an Earth-Moon L_2 (EML2) halo orbit and landers on the far side of Moon using inter-satellite ranging. However, that technique is applicable for non-maneuvering objects. For real-time positioning of maneuvering objects, such as the lander performing pinpoint landing, multiple reference points are required. Referring to the GPS technique, PHOEBE involves four CubeSats in an EML2 halo orbit to provide the references. The averages are:

1) EML2 halo orbits can always be seen from the Earth and the far side of the Moon, which is favorable for constant communication as well as tracking.

* Assistant Researcher, 9 Dengzhuang S Rd, hongru.chen@hotmail.com

2) CubeSats are miniature and fully functional, and thus can be easily carried by a mother spacecraft along with a lander going to the Moon.

For instance, ESA's AIM mission is planned to rendezvous the binary asteroid 65803 Didymos and then deploy a lander and two or more CubeSats to perform inter-satellite network [6]. It is reasonable to believe that deploying CubeSats to perform cooperative operations is a promising manner in future space missions.

To support positioning service, it is required that the four CubeSats form a favorable configuration. The limited propulsion capability of CubeSats significantly constrains trajectory options. There have been many studies (e.g. Refs. [7-9]) on the design of low- Δv transfer trajectories based on the invariant manifold associated with libration-point orbits. Folta et al [10] and Mathur [11] have studied the transfer trajectories suitable for lunar CubeSats. However, to form a constellation, it is not economical to launch the CubeSats one by one. This work applies the three-body dynamics to the design of deployment trajectories.

This Note is organized as follows. Sec. II briefly presents the model of the circular restricted three-body problem, halo orbit and invariant manifold. Sec. III gives an overview of the PHOEBE mission, including the requirement for deploying the CubeSats along a halo orbit as evenly as possible. Sec. IV discusses the methods of designing phasing trajectories for deployment. Three approaches, namely, two-impulsive correction maneuvers, patched manifolds and combination of manifolds and symmetric connecting trajectories, are presented. Conclusions are given in Sec. V.

II. System Dynamics

A. Equations of Motion

Trajectories are considered in the Earth-Moon circular restricted three-body problem (CR3BP). The CR3BP assumes that two primary bodies m_1 and m_2 are moving in a circular orbit about their barycenter. The mass of the third body is negligible compared to the masses of the two primaries. The rotating coordinate system with the origin at the barycenter, x axis along the vector between the primaries, and the z axis parallel to the rotating direction of the primary system is chosen to describe the motion of the third body. For convenience, the model is normalized by setting the angular velocity of the rotating frame, the sum of the masses of the primaries, and the distance between the two primaries to be units. Let LU represent the length unit and TU the time unit in this system. μ is the ratio of the mass of m_2 to the mass of m_1 ($\mu = 0.0122$ for the Earth-Moon system). Then, masses of m_1 and m_2 become $1-\mu$ and μ in the

normalized model. The coordinates of m_1 and m_2 become $[-\mu, 0, 0]$ and $[1-\mu, 0, 0]$, respectively, as depicted in Fig. 1.

The equations of motion of the third body are:

$$\ddot{x} - 2\dot{y} = \partial U / \partial x \quad (1)$$

$$\ddot{y} + 2\dot{x} = \partial U / \partial y \quad (2)$$

$$\ddot{z} = \partial U / \partial z \quad (3)$$

where the gravitational potential U in the system is

$$U = (x^2 + y^2)/2 + (1-\mu)/r_1 + \mu/r_2 \quad (4)$$

where

$$r_1 = \sqrt{(x+\mu)^2 + y^2 + z^2}, r_2 = \sqrt{(x-1+\mu)^2 + y^2 + z^2} \quad (5)$$

In addition, Eqs. (1)- (3) indicate a symmetry about the x - z plane. To be specific, if a set $(x, y, z, \dot{x}, \dot{y}, \dot{z}, \ddot{x}, \ddot{y}, \ddot{z}, t)$ is a solution to the equations of motion, the set $(x, -y, z, -\dot{x}, \dot{y}, -\dot{z}, \ddot{x}, -\ddot{y}, \ddot{z}, -t)$ is also a solution.

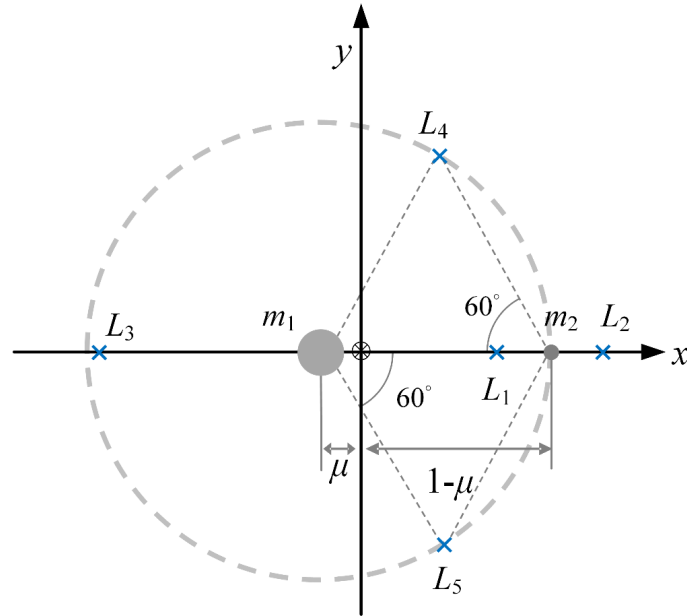


Fig. 1. Rotating frame of CR3BP and equilibrium points L_1, L_2, \dots, L_5 .

B. Halo Orbits and Invariant Manifolds

The CR3PB has five equilibrium points where velocity and acceleration are zero. They are also termed libration points or Lagrangian points labeled as L_1, \dots, L_5 . Their geometries are depicted in Fig. 1 (for details of resolving the equilibrium points, see Ref. [12]). The halo orbit is a three-dimensional periodic orbit around a collinear point, L_1, L_2 , or L_3 . Halo orbits can be computed using numerical differential correction [13]. Fig. 2 shows a group of EML2 halo orbits. The period of an Earth-Moon L_1/L_2 halo orbit is around 15 days.

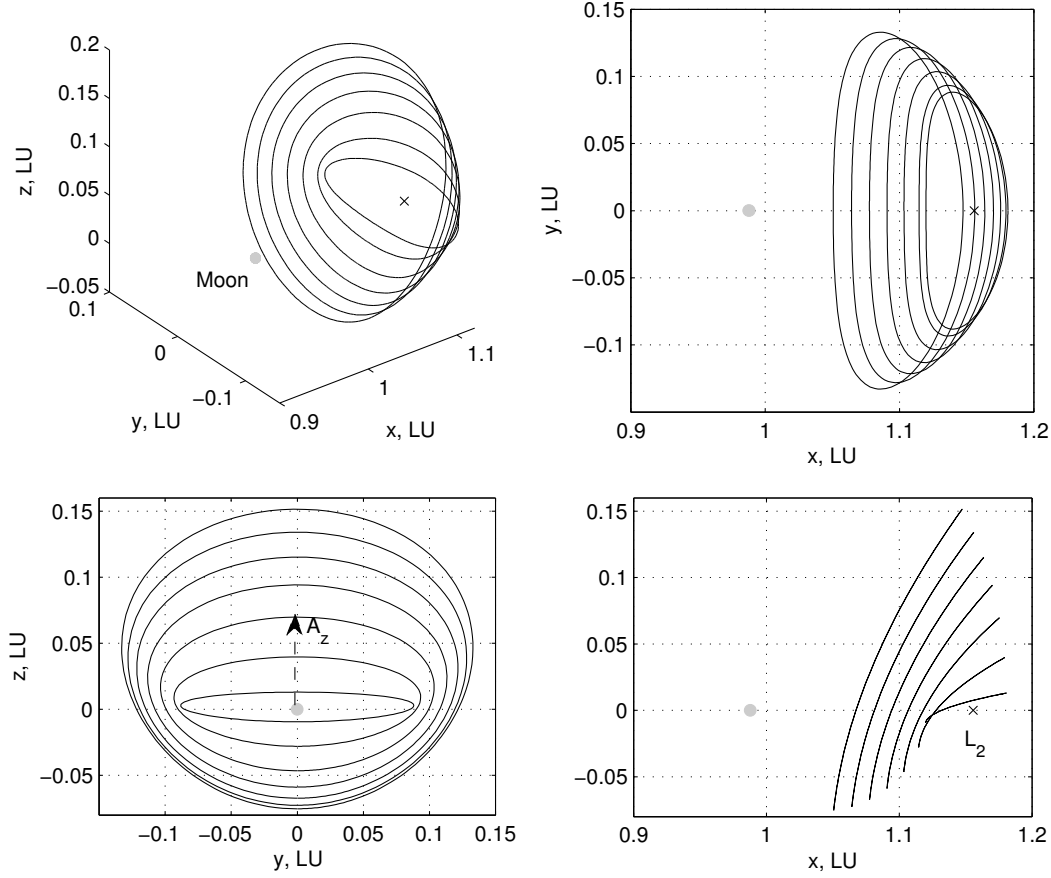


Fig. 2. Earth-Moon L_2 halo orbits.

There are a stable invariant manifold and an unstable invariant manifold associated with a halo orbit. Invariant manifolds are generated based on the eigenvectors of the monodromy matrix. The monodromy matrix is the state transition matrix for one period of a periodic orbit. For a halo orbit, it has a pair of eigenvalues λ_1 and λ_2 with $\lambda_1 > 1$, $\lambda_2 < 1$, and $\lambda_1 \lambda_2 = 1$. If a small displacement is placed along the eigenvector of the eigenvalue λ_1 , it will grow exponentially downstream. The resulting divergent trajectory is along the unstable manifold associated with the halo orbit. Conversely, backward propagating the states perturbed in the eigenvector of λ_2 yields a stable manifold that

asymptotically converges into the halo orbit. Fig. 3 shows the stable and unstable manifold trajectories derived from the Earth-Moon L_2 halo orbit with z -amplitude $A_z = 15,000$ km.

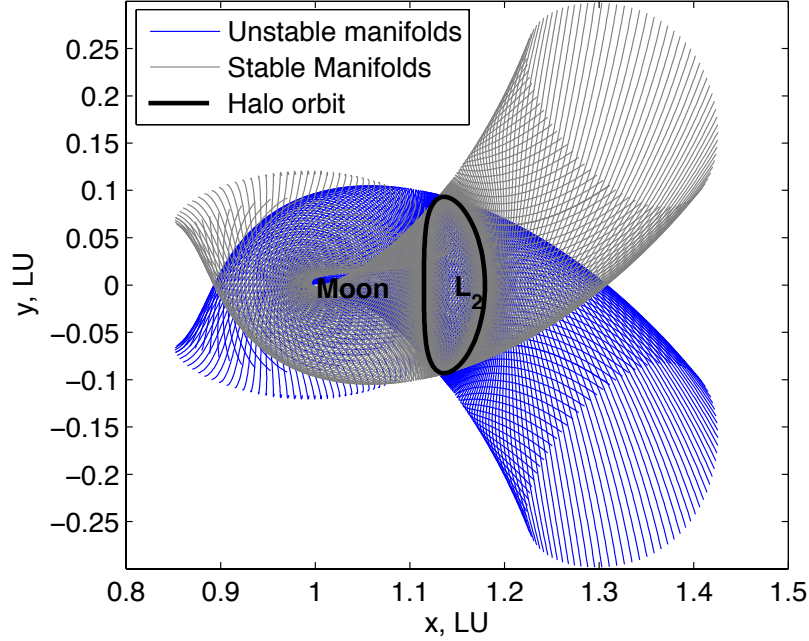


Fig. 3. An EML₂ halo orbit and the stable and unstable manifolds associated with it.

C. Parameterization

Invariant manifolds can be used as the pathway to send spacecraft from or to the halo orbit at little Δv cost. In this work, invariant manifolds instead of the halo orbit are the initial and final conditions of the trajectory design. For the concerned optimization problem, the manifold and halo orbit should be parameterized. Let T denote the period of the halo orbit, and τ ($0 \leq \tau < T$) denote the time past a reference point in the halo orbit. The x - z plane crossing on the far side was taken as the reference point for this work. Δv are added at different points defined by τ to generate manifold trajectories. The Δv direction is chosen to be equivalent to the divergent eigenvector or convergent eigenvector (for details, see Ref. [14]). Magnitudes of departure and insertion Δv are all set to be 1 cm/s. Then, the manifold trajectory can be uniquely specified by τ .

III. Problem Statement

The EML2 is 64,500 km from the Moon. The halo orbits around EML2 are visible to both the Earth and the far side of the Moon. Moreover, the directions of the lines of sight to the Earth and the Moon are almost aligned, which is favorable for communication as well as attitude control. The PHOEBE project is to deploy four 6U CubeSats along an EML2 halo orbit to support the positioning of users on the far side of the Moon (see Fig. 4).

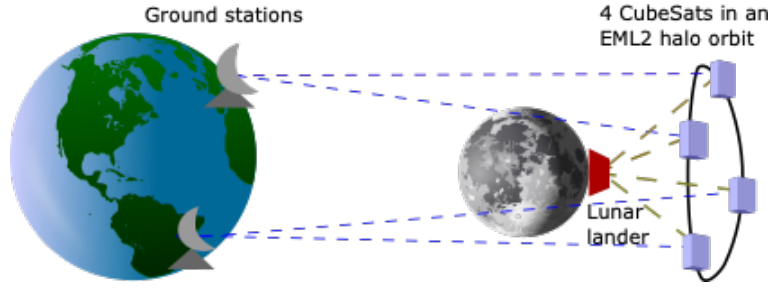


Fig. 4. Schematic of tracking CubeSats and lunar landers on the far side.

The positions of the CubeSats are determined by processing the ranging data from the ground stations on Earth. With the positions of the CubeSats known, through ranging between the user on the far side of the Moon and the CubeSats, the user can resolve its position through a proper estimation algorithm. The position error ($\Delta position$) of the user can be expressed as the product of the pseudorange error ($\Delta pseudorange$) and a geometric index; that is,

$$\Delta position = GDOP \times \Delta pseudorange \quad (6)$$

where GDOP (Geometric Dilution of Precision) is related to the configuration of the CubeSats with respect to the user. GDOP can be computed from,

$$\mathbf{H} = \begin{bmatrix} \frac{(x_1 - x)}{R_1} & \frac{(y_1 - y)}{R_1} & \frac{(z_1 - z)}{R_1} & -1 \\ \frac{(x_2 - x)}{R_2} & \frac{(y_2 - y)}{R_2} & \frac{(z_2 - z)}{R_2} & -1 \\ \frac{(x_3 - x)}{R_3} & \frac{(y_3 - y)}{R_3} & \frac{(z_3 - z)}{R_3} & -1 \\ \frac{(x_4 - x)}{R_4} & \frac{(y_4 - y)}{R_4} & \frac{(z_4 - z)}{R_4} & -1 \end{bmatrix} \quad (7)$$

$$GDOP = \sqrt{Tr(\mathbf{H}^T \mathbf{H})^{-1}} \quad (8)$$

where x, y and z denote the position of the user, x_i, y_i and z_i denote the position of the i -th CubeSat, and R_i denotes the distance between the user and the i -th CubeSat. The smaller the GDOP is, the better the configuration is for positioning. With no influence of atmosphere on the Moon, $\Delta pseudorange$ is considered mainly contributed by the error of orbit determination of the CubeSats. According to orbit determination result of ARTEMIS [15], $\Delta pseudorange$ is assumed to be 20 meters. For a desirable $\Delta position$ of 1 km, GDOP should be smaller than 50.

GDOP depends on the configuration of the CubeSats. In this note, the interval between two CubeSats is represented by the difference of their phase angles, which is,

$$\Delta\phi = \Delta\tau / T \times 360^\circ \quad (9)$$

where $\Delta\tau$ is the difference between the τ of two CubeSats in the halo orbit. Then, $\Delta\phi$ is associated with $\Delta\tau$. Fig. 4 shows the configurations with different $\Delta\phi$ between neighboring CubeSats and different A_z of halo orbits, and the corresponding GDOP in a period. The GDOP for the same $\Delta\phi$ does not change too much with A_z . However, GDOP is greatly depending on $\Delta\phi$. Without doubt, the best configuration is that they are evenly spaced along the halo orbit; namely, they are separated evenly by a phase angle difference $\Delta\phi = 90^\circ$. As indicated in the figure, the $GDOP < 50$ holds for 86% of the time for this case, which means the positioning performance is satisfactory for 86% of the time. In addition, a working interval lasts 3.2 days, and a blackout interval lasts 0.5 day. As the period of a low lunar orbit (e.g. 2 hours for an orbit with an altitude of 100 km) and duration of landing (i.e. around 12 min) are comparatively short, the time waiting for a landing is not be longer than 0.5 day.

On the other hand, it is not economical to launch four CubeSats separately. Therefore, it is assumed that a mother spacecraft carries a lunar lander and four CubeSats to the Moon. In the transfer phase from the Earth to the halo orbit, the rocket and mother spacecraft can provide the required powerful boosts. However, it is infeasible for the mother spacecraft to bring four CubeSats to their different destinations one by one, as the fuel cost will be unacceptably high. Therefore, it is assumed that the CubeSats as a whole are released at the stable manifold heading for the halo orbit at once. Then, the CubeSats are distributed into different phase angles of the halo orbit using their propulsion systems. Constrained by size, CubeSats have limited propulsion capacity. Therefore, it is needed to design the phasing trajectories that require affordable Δv .

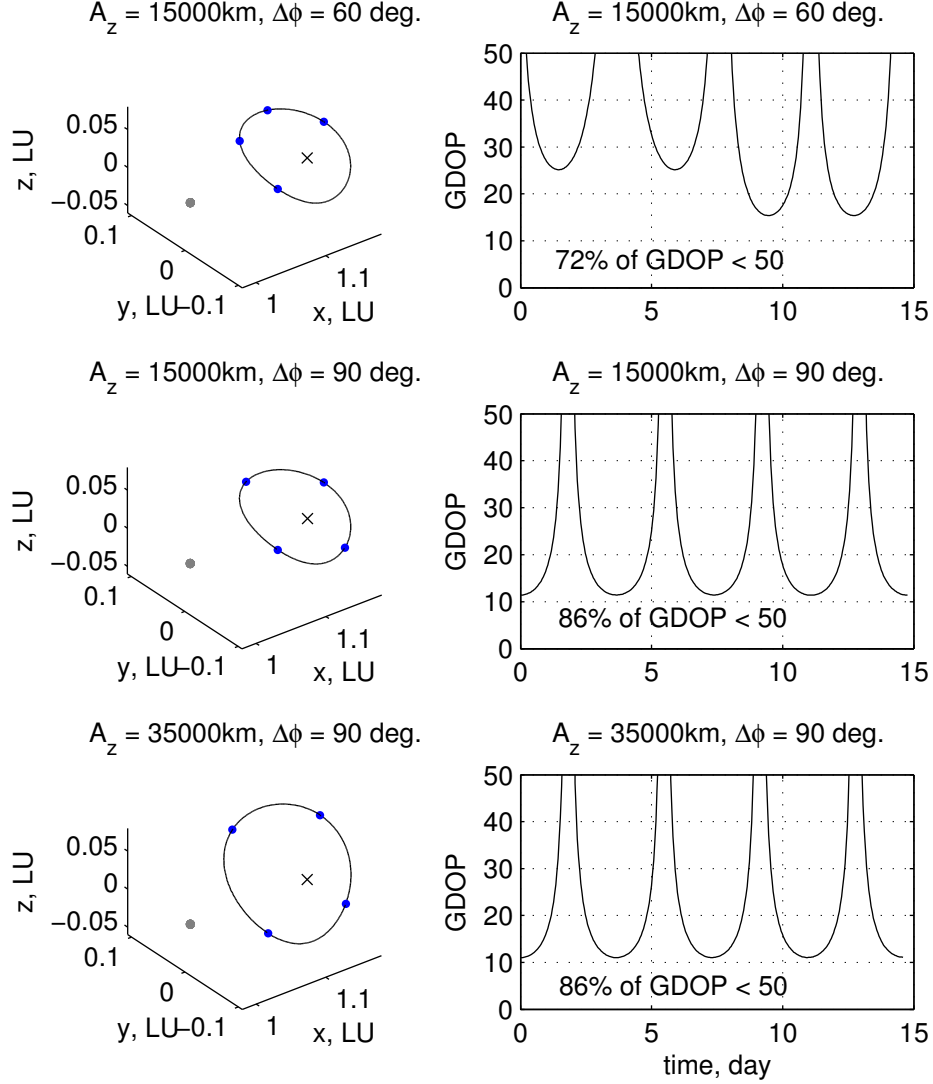


Fig. 5. Different configurations and the corresponding GDOP.

IV. Phasing Trajectory Design

a. Two-impulsive Correction Maneuvers

The halo orbit with $A_z = 15,000\text{ km}$ is taken for the case study hereafter. The CubeSats are released at an initial stable manifold trajectory associated with the halo orbit. Applying maneuvers can send the CubeSats into another stable manifold trajectory whose τ is $\Delta\tau$ from the initial τ_0 . The two-impulsive correction maneuver is the most common way to correct a trajectory. The first maneuver Δv_1 is to deliver the CubeSat to meet a position along the target manifold trajectory, and the second maneuver Δv_2 is to cancel the velocity mismatch at the patch point. In summary, for a specified $\Delta\phi$, the optimization program is to solve for the independent variables, namely, τ_0 , departure

epoch, t_1 , Δv_1 at t_1 , arrival epoch t_2 , and Δv_2 at t_2 , such that the trajectory state meets the target trajectory state after t_2 and the total Δv (i.e. $\Delta v_1 + \Delta v_2$) is a minimum. Optimization is done with the MATLAB fmincon routine. Multiple initial guesses of t_1 and t_2 are tried.

Table 1 lists the minimum Δv for various $\Delta\phi$. Fig. 6 shows an example of changing the manifold trajectory to the one (blue) with a $\Delta\phi$ of -120° from the initial (black). To form the best configuration, it is necessary to acquire a $\Delta\phi$ of $+180^\circ$ or -180° . However, the required Δv of 240 m/s is far beyond the capacity of a CubeSat.

Table 1. Minimum Δv for different $\Delta\phi$ using two-impulsive correction maneuvers.

$\Delta\phi$, deg.	Δv , m/s
± 180	240
± 120	190
± 90	170
± 60	120
± 30	55

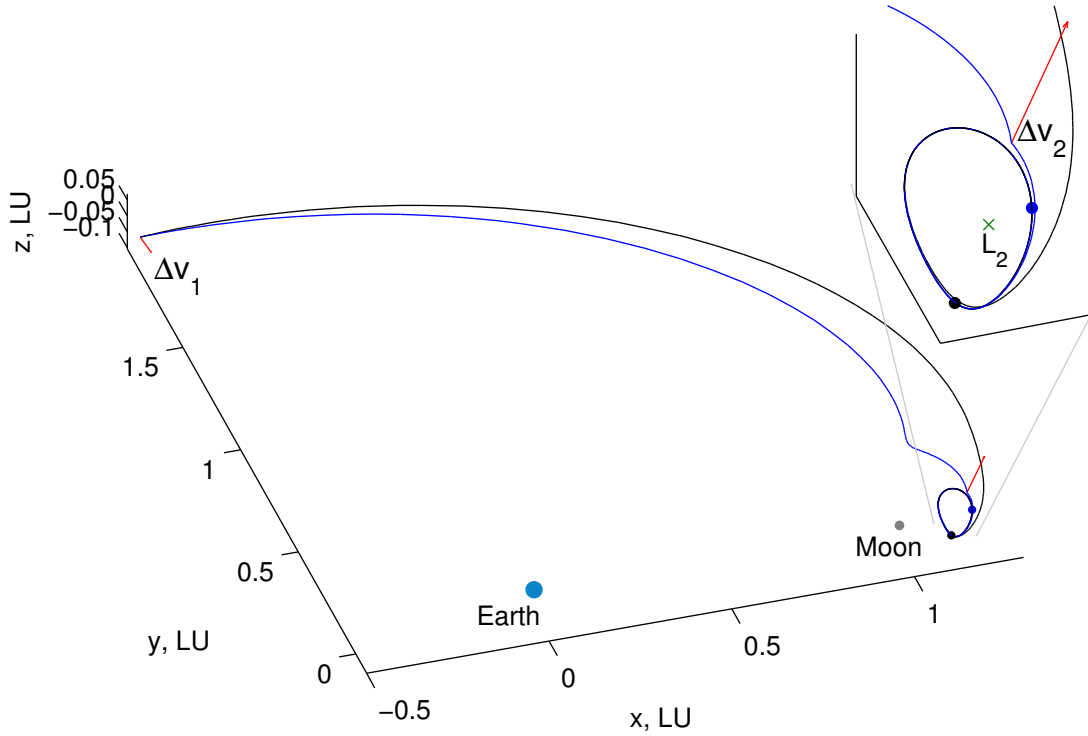


Fig. 6. Two-impulsive correction maneuvers (arrow) to cause a $\Delta\phi$ of -120 deg.

b. Patched Manifolds

By observing Fig. 3, one can notice that the Moon-ward manifolds are turned by the lunar gravity when close to the Moon. Recalling the symmetry of the CR3BP, the unstable manifold and stable manifold completely match at $y = 0$ in position (see Fig. 2). However, the velocity difference at $y = 0$ is not zero. If a Δv is paid to cancel that velocity mismatch, the CubeSat can go through the unstable and stable manifolds, and back in the halo orbit resulting in a $\Delta\phi$. According to the symmetry, $\Delta v = 2\sqrt{v_x^2 + v_z^2}$, where v_x and v_z are the x - and z - components of the velocity of the manifolds crossing the x - z plane, respectively. $\Delta\phi$ is due to the additional time spent on the transfer along the manifolds. Let τ_0 represents the τ of the departure manifold trajectory. Then, $T - \tau_0$ is the τ of the insertion manifold trajectory because of the symmetry. $\Delta\phi$ is computed from,

$$\Delta\phi = \text{rem}(T - 2\tau_0 - \text{ToF}, T) / T \times 360^\circ \quad (10)$$

where ToF is the flight time from leaving the halo orbit to insertion to the halo orbit. As new phase angles lag the initial phase angle, negative values are used for $\Delta\phi$. Fig. 7 displays the manifolds on the Poincare section of $y = 0$, along with the corresponding Δv and $\Delta\phi$ measured by the color scale.

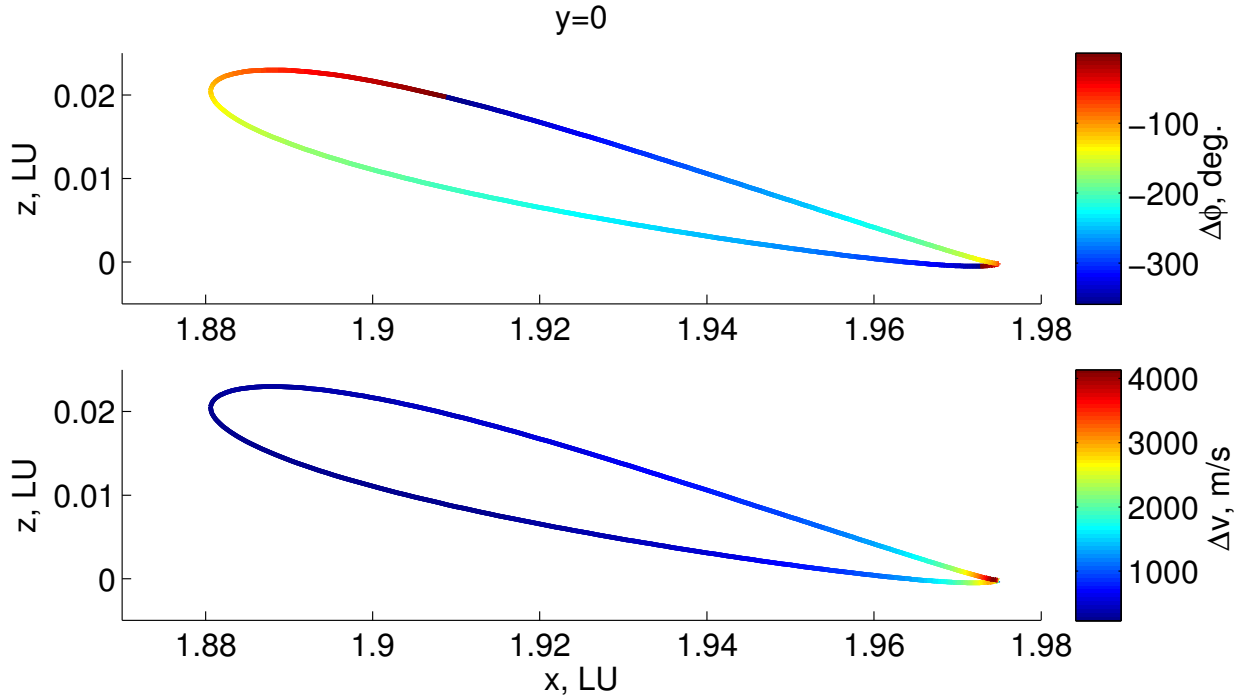


Fig. 7. Manifolds on the Poincare section of $y = 0$, along with Δv and $\Delta\phi$.

Fig. 8 shows the relationship between Δv and $\Delta\phi$. There are two lines because phase angles repeat every period of the halo orbit. The minimum Δv is 250 m/s at $\Delta\phi = -180^\circ$. The order of the Δv for different $\Delta\phi$ is larger than that of using two-impulsive correction maneuvers. However, since only one Δv is applied in this method, $\Delta\phi$ cannot be freely changed. In other words, Δv is naturally associated with $\Delta\phi$. Some modification is made in the next subsection to gain a flexibility of changing $\Delta\phi$ as well as the minimum required Δv .

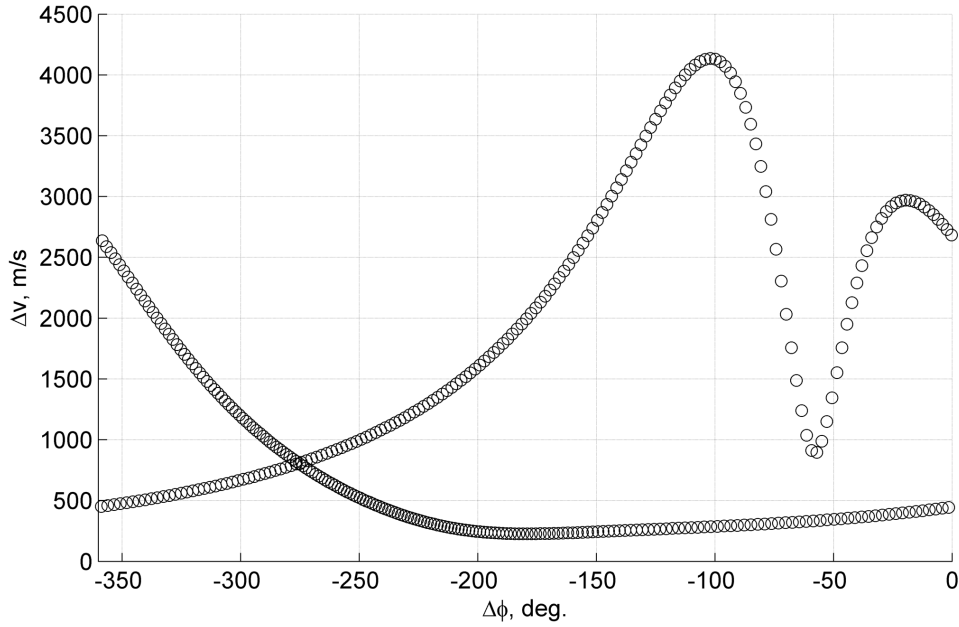


Fig. 8. Δv vs $\Delta\phi$ for patched manifold trajectories.

c. Symmetric connecting trajectories

Neither the correction maneuvers applied in the transfer phase prior to the halo orbit, nor the manifold patch on the Moon side can achieve the desired configuration with affordable Δv . To take advantage of the lunar gravity, the unstable and stable manifolds on the Moon side are still used in this subsection. Recalling the symmetry property, if a $\Delta \mathbf{v}_1$ (i.e., $[\Delta v_x, \Delta v_y, \Delta v_z]^T$) is placed along the Moon-ward unstable manifold before an x - z plane crossing, such that v_x and v_z will be zero at the crossing, the resulting trajectory after the crossing will mirror the trajectory before, and hence goes back to the stable manifold as well as the. Another $\Delta \mathbf{v}_2$ (i.e., $[-\Delta v_x, \Delta v_y, -\Delta v_z]^T$) that is symmetric to $\Delta \mathbf{v}_1$ is needed for the insertion to the stable manifold trajectory that is also symmetric to the departure unstable manifold trajectory.

Recalling Eq. (10), by varying the flight time (i.e. $ToF/2$) to arrive at $[v_x, v_z, y]^T = [0, 0, 0]^T$, $\Delta\phi$ can be altered. For a specified $\Delta\phi$, the optimization program is to find the independent variables, namely, τ_0 of the departure manifold trajectory, t_1 when $\Delta\mathbf{v}_1$ is placed, and $\Delta\mathbf{v}_1$, such that v_x, v_z and y are zero $ToF/2$ after leaving the halo orbit and $\Delta\mathbf{v}_1$ is a minimum. Because $\Delta\mathbf{v}_1$ is minimized, the total $\Delta\mathbf{v}$ (i.e. $\Delta\mathbf{v}_1 \times 2$) is also minimized. Again, the optimization is done with the MATLAB `fmincon` routine. Multiple initial guesses of τ_0 and t_1 are tried to ensure a global optimality.

Fig. 9 shows the minimum $\Delta\mathbf{v}$ vs $\Delta\phi$. The figure exhibits several Pareto fronts. By investigation, they are found associated with different types of trajectories. When $\Delta\phi$ is close to 0 or $\pm 360^\circ$, the optimal phasing trajectories stay close to the halo orbit, as indicated in the figure. This type of trajectory is referred to as Type 1. The $\Delta\mathbf{v}$ associated with Type 1 increases readily with $|\Delta\phi|$ and $360^\circ - |\Delta\phi|$. The trajectories touring the Moon (Type 2) require lower $\Delta\mathbf{v}$ for larger $|\Delta\phi|$ and $360^\circ - |\Delta\phi|$. For Type 2, the minimum $\Delta\mathbf{v}$ is generally above 100 m/s. Results in Fig. 8 are found within the interval $ToF < 50$ days. If the maximum ToF is extended by one period of the halo orbit, the same $\Delta\phi$ recur. Longer flight time suggests that a small $\Delta\mathbf{v}$ can make an influential difference. Fig. 10 shows the results within the interval $ToF \in [50, 75]$ days. It can be seen that, with additional flight time, optimal trajectories can reach to as far as L_1 (Type 3). Type-3 trajectories can achieve a wide range of $\Delta\phi$ with $\Delta\mathbf{v}$ smaller than 100 m/s. In addition, Figs. 9, 10 show disconnected profiles for Type 2. These different profiles are associated with different types of Type-2 trajectories; namely, different numbers of revolutions about the Moon and EML2.

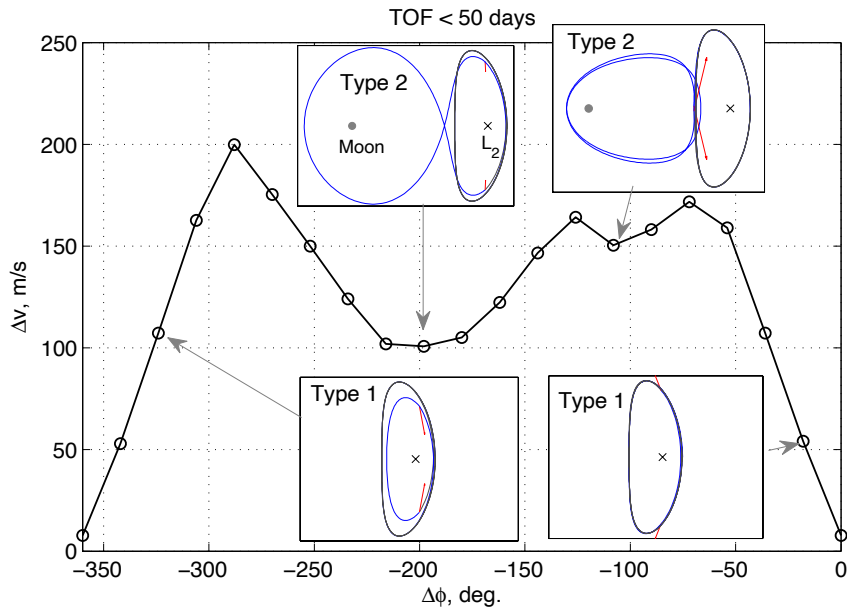


Fig. 9. Minimum $\Delta\mathbf{v}$ vs $\Delta\phi$ for the phasing using symmetric connecting trajectories with $ToF < 50$ days.

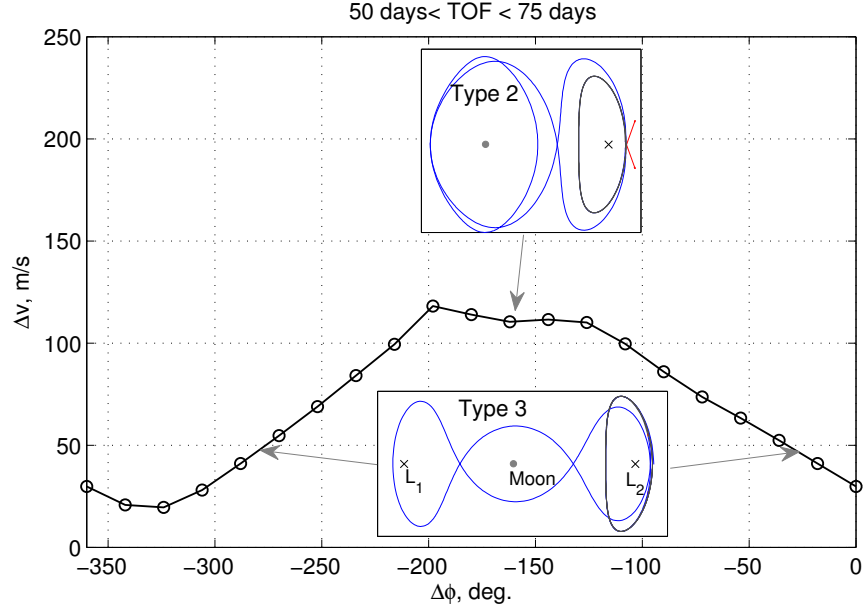


Fig. 10. Minimum Δv vs $\Delta \phi$ for the phasing using symmetric connecting trajectories with $ToF \in [50, 75]$ days.

To achieve even distribution with minimized required Δv for one CubeSat, it is decided to deploy the four CubeSats to the phase angles that are -20° , -110° , -200° and -290° from the initial orbit. The Δv are 55, 99, 101 and 42 m/s, respectively (see Fig. 9 and Fig. 10). Hence, the maximum required Δv for one CubeSat is 101 m/s. Fig. 11 shows the corresponding phasing trajectories. As demonstrated, starting from the same point in the halo orbit at time $t = 0$, the four CubeSats are distributed evenly along the halo orbit in 58 days.

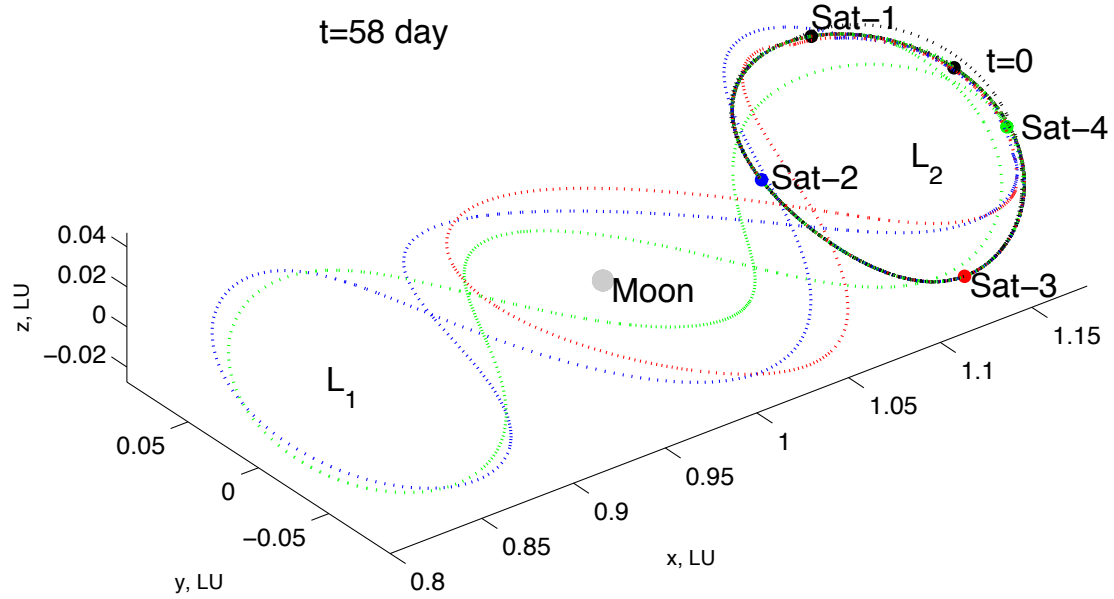


Fig. 11. Phasing trajectories (dashed) to deploy four CubeSats evenly along the halo orbit (solid black).

d. Discussions

By investigation, it is found that a cold gas propulsion system for CubeSats with a mass of 3.5 kg (estimated propellant mass around 1.93 kg) can provide a total impulse of 750 N-sec[†]. The designed PHOEBE CubeSat without a propulsion system has a mass of 4.7 kg. Consequently, a Δv budget of 105 m/s is available, which can meet the requirement of deployment.

The method of forming symmetric connecting trajectory can be regarded as a special case of the two-impulsive correction method. The specialty is that it takes advantage of the symmetry property and lunar gravity to simplify the trajectory design. The symmetric connecting trajectory is similar to the “bridging trajectory” demonstrated by Davis et al. [9] in the sense that they both connect unstable and stable manifold trajectories. The difference is that the symmetric connecting trajectory can be used for the transfer starting and arriving at the same libration-point orbit, while the bridging trajectory can be used for the transfer between a L_1 orbit and an L_2 orbit. In addition, the process of deployment is reverse to the process of rendezvous. Sato et al. [16] have optimized low-thrust trajectories for the

[†] <http://www.cubesat-propulsion.com/jpl-marco-micro-propulsion-system/>, accessed October 2 2016.

rendezvous of two spacecraft in the same halo orbit. While they did not impose the constraint of symmetry, their optimal trajectories for large initial $\Delta\phi$ also tour the Moon and exhibit symmetry about the x - z plane. That implies the optimal symmetric trajectories solved in the previous subsection are of global optimality, and the present method can be applied to rendezvous missions as well.

Although the Earth-Moon CR3BP is a simplified model without considering the eccentricity of Moon's orbit and other perturbations such as solar radiation pressure, the conclusions obtained in this model are considered reliable to the real world. The presented method can be applied to high-fidelity models with minor modification (usually through correction Δv).

V. Conclusion

It is desirable to deploy four CubeSats along an Earth-Moon L_2 halo orbit to provide positioning service for users on the far side of the Moon. In this Note, the deployment trajectories that apply two-impulsive correction maneuvers, patched manifolds and symmetry of the three-body problem have been investigated. The result indicates that the combination of manifolds and symmetric connecting trajectories can lead to various phase angle differences with relatively low Δv . These phasing trajectories can be used for forming constellations in a halo orbit. It is obtained that a Δv around 100 m/s is needed to deploy four CubeSats evenly along the halo orbit (corresponds to a positioning accuracy of 1 km on the surface of the Moon). Three types of phasing trajectories, namely, around the halo orbit, touring the Moon and touring the Earth-Moon L_1 point, are involved in the deployment. A modern CubeSat propulsion system can meet the Δv requirement. Moreover, this phasing method can be applied to not only constellation deployment, but also rendezvous in a three-body system.

Acknowledgments

This work is supported by the National Natural Science Foundation of China (grant 11372311) and the Advanced Study Program (grant CSU-QZKT-201711) of Technology and Engineering Center for Space Utilization, Chinese Academy of Sciences. The authors wish to thank Yang Gao for the support of the PHOEBE project, Wenbin Wang and Jiangkai Liu for their comments on navigation problems.

References

- [1] Chen, H., Meng, Y., and Ma, J., "Phasing Trajectories for a CubeSat Lunar Far-side Positioning Mission",

26th Workshop on Astrodynamics and Flight Mechanics, ISAS/JAXA, Jul. 25-26, 2016.

- [2] Burns, J. O., Kring, D. A., Hopkins, J. B., Norris, S., Lazio, T. J. W., and Kasper, J., “A Lunar L2-Farside Exploration and Science Mission Concept with the Orion Multi-Purpose Crew Vehicle and a Teleoperated Lander/rover,” *Advances in Space Research*, vol. 52, 2013, pp. 306–320. doi:10.1016/j.asr.2012.11.016
- [3] Li, F., Zhange, H., Wu, X., Ma, J., and Zhou, W., “The Science Value and Technical Challenge of Chang’E-4 Landing on the Far-side of the Moon,” 41st COSPAR Scientific Assembly, Abstract No. B0.1-18-16, Istanbul, Turkey, July 2016.
- [4] Hill, K., and Born, G. H., “Autonomous Interplanetary Orbit Determination Using Satellite-to-Satellite Tracking,” *Journal of Guidance, Control, and Dynamics*, vol. 30, 2007, pp. 679–686. doi:10.2514/1.24574
- [5] Hesar, S. G., Parker, J. S., Leonard, J. M., McGranaghan, R. M., and Born, G. H., “Lunar far side surface navigation using Linked Autonomous Interplanetary Satellite Orbit Navigation (LiAISON),” *Acta Astronautica*, vol. 117, 2015, pp. 116–129. doi:10.1016/j.actaastro.2015.07.027
- [6] Koppers, M., Carnelli, I., Galvez, A., Mellab, K., Michel, P., and the AIM team, “The Asteroid Impact Mission (AIM),” European Planetary Science Congress, Abstract No. EPSC2015-162, 2015.
<http://meetingorganizer.copernicus.org/EPSC2015/EPSC2015-162-1.pdf>
- [7] Koon, W.S., Lo, M. W., Masden, J.E., and Ross, S.D., “Low Energy Transfer to the Moon”, *Celestial Mechanics and Dynamical Astronomy*, vol. 81, 2001, pp.63–73.
- [8] Gómez, G., Koon, W.S., Lo, M.W., Marsden, J.E. Ross, S.D., “Connecting orbits and invariant manifolds in the spatial restricted three-body problem”, *Nonlinearity*, vol. 19, no. 5, 2004, pp. 1571-1606. doi: 10.1088/0951-7715/17/5/002
- [9] Davis, K.E., Anderson, R.L., Scheeres, D.J., and Born, G.H., “The Use of Invariant Manifolds for Transfers Between Unstable Periodic Orbits of Different Energies”, *Celestial Mechanics and Dynamical Astronomy*, vol. 107, 2010, pp. 471-485. doi: 10.1007/s10569-010-9285-3
- [10] Folta, D., Dichmann, D., Clark, P., Haapala, A. F., and Howell, K., “Lunar Cube Transfer Trajectory Options,” AAS/AIAA Space Flight Mechanics Meeting, Williamsburg, VA, Jan. 11-15, 2015, Paper No. AAS 15-353, *Advances in the Astronautical Sciences*, vol. 155, Furfaro, R., Casotto, S., Trask, A. and Zimmer, S. (ed.), San Diego, Univelt, 2015.
- [11] Mathur, R., “Low Thrust Trajectory Design and Optimization: Case Study of a Lunar CubeSat Mission,” 6th

International Conference on Astrodynamics Tools and Techniques, Darmstadt, Germany, Mar. 14-17, 2016.

<https://indico.esa.int/indico/event/111/session/21/contribution/150/material/paper/0.pdf>

- [12] Szebehely, V., *Theory of Orbits: The Restricted Problem of Three Bodies*, New York, San Francisco, London, Academic Press, 1967, pp. 134-139.
- [13] Howell, K. C., “Three-Dimensional, Periodic, ‘Halo’ Orbits,” *Celestial Mechanics*, vol. 32, 1984, pp. 53-71.
- [14] Gomez, G., Howell, K., Masdemont, J., and Simo, C., “Station-keeping strategies for translunar libration point orbits”, AAS/AIAA Astrodynamics Specialist Conference, Monterey, California, Feb. 9-11, 1998, Paper No. AAS 98-168, *Advances in the Astronautical Sciences*, vol. 99, Middour, J. W., Sackett, L.L., D'Amario, L., and Byrnes, D. V. (ed.), Univelt, 1998, pp. 949–967.
- [15] Woodard, M. A., Cosgrove, D., Morinelli, P., Marchese, J., Owens, B., and Folta, D. C., and “Orbit Determination of Spacecraft in Earth-Moon L1 and L2 Liberation Point Orbits,” AAS/AIAA Astrodynamics Specialist Conference, August 1-4, 2011, Girdwood, Alaska, Paper No. AAS 11-514, *Advances in the Astronautical Sciences*, vol. 142, Schaub, H., Gunter, B. C., Russell, R. P., and Cerven, W. T. (ed.), San Diego, Univelt, 2012, pp. 1701–1714.
- [16] Sato, Y., Kitamura, K., and Shima, T., “Spacecraft Rendezvous Utilizing Invariant Manifolds for a Halo Orbit”, *Transactions of the Japan Society for Aeronautical and Space Sciences*, vol. 58, No. 5, 2015, pp. 261-269.